J Mater Sci (2007) 42:752–758
DOI 10.1007/s10853-006-1447-z

Preparation and electrochemical characteristics of microemulsion-derived Li(Ni, Co)O_2 nanopowders

Chung-Hsin Lu · Hsien-Cheng Wang

Received: 1 March 2004 / Accepted: 13 April 2006 / Published online: 12 January 2007

Abstract Nanosized $LiNi_{0.9}Co_{0.1}O_2$ powders used in lithium-ion batteries are successfully prepared via a water-in-oil microemulsion process. The average particle sizes of the microemulsion-derived $LiNi_{0.9}Co_{0.1}O_2$ powders are in nanometer scale. The obtained powders are much smaller in size than the specimens prepared via the conventional solid state and sol–gel processes. Oxygen has significant enhancement effects on the cationic ordering of the calcined powders. Highly cation-ordered $LiNi_{0.9}Co_{0.1}O_2$ powders with a layered $R\bar{3}m$ structure are obtained after heat-treatment at 800 °C in O_2. In addition, the high intensity ratio of I_{003}/I_{104} reveals that lithium ions and transition metal ions are regularly situated at the 3a and 3b sites, respectively, rendering the high cationic ordering. The discharge capacity of the first cycle for the specimen calcined at 800 °C in O_2 is 170.9 mAh/g. After 20 cycles, the capacity retention of $LiNi_{0.9}Co_{0.1}O_2$ powders is 93.2%, indicating that $LiNi_{0.9}Co_{0.1}O_2$ powders with good cycling characteristics are obtained via the microemulsion process.

Introduction

Lithium-ion secondary batteries are being viewed as the primary energy system for portable electronic devices. In order to improve the electrochemical performance of lithium-ion secondary batteries, intensive efforts have been devoted in developing several lithiated transition metal oxides including $LiNiO_2$ [1, 2], $LiMn_2O_4$ [3, 4], $LiMnO_2$ [5, 6], and Li(Ni,Co)O_2 [7–9]. The isostructural lithiated oxide-Li(Ni, Co)O_2 has been widely investigated, owing to its high discharge capacity and relatively low material cost compared with $LiCoO_2$. The crystal structure of Li(Ni, Co)O_2 oxides is categorized as the α-$NaFeO_2$ type, which has a rhombohedral $R\bar{3}m$ symmetry. This compound is superior to $LiCoO_2$ in terms of its high practical discharge capacity. In addition, partial substitution of cobalt ions in Li(Ni,-Co)O_2 restrains the disorder among lithium and nickel ions, leading to an improvement of the electrochemical performance [10, 11].

Recently, certain soft-chemistry processes including the sol–gel method and the co-precipitation route are utilized for preparing Li(Ni, Co)O_2 with improved cycling performance [12–14]. However, prolonged calcination at elevated temperatures is still required in these processes. The water-in-oil (W/O) microemulsion technique is one of the potential routes for synthesizing nanosized powders in short reaction time. The W/O microemulsion is optically transparent and thermodynamically stable [15, 16]. A W/O microemulsion system is composed of a continuous oil phase and an aqueous phase that are compartmentalized by a surfactant phase to form nanosized liquid droplets [17]. These droplets provide a specific microenvironment for the reactants to be mixed thoroughly in atomic scale [18, 19]. As a result, the high homogeneity directly facilitates the chemical reaction to form nanosized powders within short reaction time. In this study, a W/O microemulsion technique is developed to synthesize

C.-H. Lu (✉) · H.-C. Wang
Electronic and Electro-optical Ceramics Laboratory, Department of Chemical Engineering, National Taiwan University, Taipei, Taiwan, R.O.C.
e-mail: chlu@ccms.ntu.edu.tw

$LiNi_{0.9}Co_{0.1}O_2$ nanopowders. The exothermic/endothermic behaviors and weight loss of the reactants are characterized. The structural development and morphological evolution of the calcined powders are analyzed. The electrochemical characteristics of the calcined $LiNi_{0.9}Co_{0.1}O_2$ powders at ambient temperature are also investigated.

Experimental

For preparing the microemulsion solutions, reagent grade lithium nitrate, cobalt nitrate, and nickel nitrate were dissolved in deionized water to form the aqueous phase. The concentration of total cations in the aqueous phase was set to be 1 M, and the molar ratio of Li^+:Ni^{2+}:Co^{2+} was fixed at 1:0.9:0.1 for synthesizing the desired $LiNi_{0.9}Co_{0.1}O_2$ powders. After mixing the reactants, a dark-brown aqueous solution was obtained and later dissolved into the mixture of continuous phase using cyclohexane as the oil phase. Polyoxyethylene (10) octylphenyl ether (OP-10) and 1-hexanol were utilized as the surfactant and co-surfactant, respectively. The volume ratio of the aqueous solution to the mixture of OP-10 and 1-hexanol was set to be 3:10. Nanosized reverse micelles were formed and stabilized with the surfactant and co-surfactant, resulting in the formation of the optically transparent microemulsion solution. The obtained microemulsion was dropped into hot kerosene to evaporate water at around 180 °C, followed by drying at 350 °C for 4 h to burn away residual organic species to obtain the precursors. These dried precursors were heated from 600 to 900 °C in air and in O_2 flows with a flowing rate of 1 L/min in tubular furnace. To understand the reaction process and weight loss of the precursors, the dried powders were subjected to the thermal analysis (DTA/TG) at a heating rate of 10 °C/min in O_2. Powder X-ray diffraction (XRD) was performed to analyze the crystal structures of the heated powders. Transmission electron microscopy (TEM) was utilized to examine the microstructures and particle sizes of the powders calcined at various temperatures.

The electrochemical characteristics of the microemulsion-derived $LiNi_{0.9}Co_{0.1}O_2$ powders were investigated in coin cells. The cathodes were prepared by mixing the 800 °C-calcined $LiNi_{0.9}Co_{0.1}O_2$ powders, carbon black, and polyvinylidene difluoride (PVDF) in a weight ratio of 85:10:5 using *n*-methyl-2-pyrrolidone (NMP) as the solvent. The thoroughly mixed slurries were coated onto Al foils and heated overnight at 120 °C in vacuum. Lithium foil was adopted as the anode, and the solution made by dissolving 1 M $LiPF_6$ in a mixture of ethylene carbonate (EC) and dimethyl carbonate (DMC) (1:1 by volume) was utilized as the electrolytes. All coin cells were assembled in a glove box filled with high-purity argon. The charging and discharging characteristics were examined galvanostatically in the potential range of 3.0–4.3 V at a current density of 54.8 mA/g (C/5 rate).

Results and discussion

Thermal behaviors of the precursors

The exothermic/endothermic behaviors and weight loss of as-dried precursors were characterized using DTA/TG from ambient temperature to 900 °C in O_2. The DTA/TG curves are depicted in Fig. 1. The weight loss occurs at around 100 °C, indicating the evaporation of the absorbed water from the surface of the precursors. The exothermic peak ranging from 350 to 500 °C in the DTA curve signifies the combustion of the residual organic species, leading to a corresponding weight loss in TG. When the heating temperature reaches 650 °C, a marked endothermic peak is observed from 650 to 750 °C. This stage refers to the formation reaction of $LiNi_{0.9}Co_{0.1}O_2$ from the precursors.

Crystal structural analysis and microstructural observation of $LiNi_{0.9}Co_{0.1}O_2$ calcined in air

To investigate the reaction processes of the $LiNi_{0.9}Co_{0.1}O_2$ precursors, the crystal structures of the

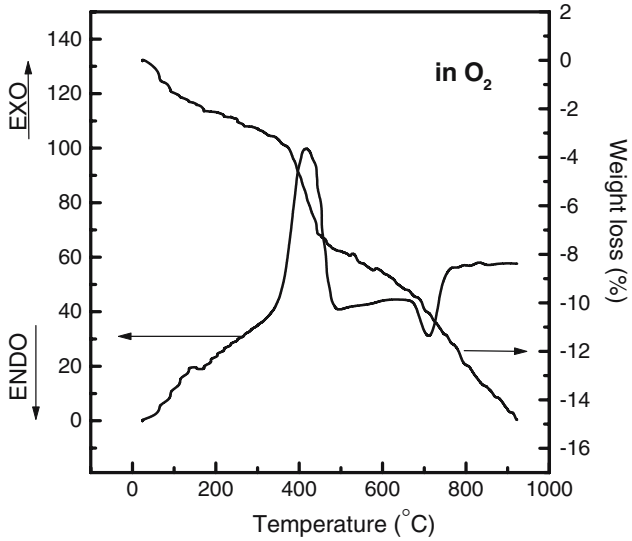

Fig. 1 DTA and TG curves of the precursors heated in O_2 prepared via the microemulsion process

specimens calcined in the range of 600–900 °C for 2 h in air were examined by XRD. Figure 2 illustrates the obtained XRD patterns for the calcined specimens. It is shown in Fig. 2(a) that the 600 °C-calcined powders are primarily composed of two phases-Li_2CO_3 and NiO. According to Fig. 2(b) and (c), pure $LiNi_{0.9}Co_{0.1}O_2$ is formed at 700 °C and 750 °C. When the calcination temperature is raised to 800 °C, the crystallinity of the obtained $LiNi_{0.9}Co_{0.1}O_2$ powders increases. Further heating the microemulsion-derived specimens at 900 °C results in the significant lowering of the (003) diffraction line (see Fig. 2e). The inset in Fig. 2 illustrates the relation between the intensity ratios of I_{003}/I_{104} and the calcination temperature. For compounds having a $R\bar{3}m$ structure, the intensity ratio of I_{003}/I_{104} can be utilized to estimate the ordering of the cations at 3a and 3b sites [20]. The intensity ratios of I_{003}/I_{104} for the specimens calcined at 700 °C and 750 °C are calculated to be 0.39 and 0.41, respectively. As the heating temperature is raised to 800 °C, the intensity ratio increases to 0.62. Once the heating temperature reaches 900 °C, the intensity ratio of I_{003}/I_{104} markedly decreases to merely 0.2. These results reveal the considerable displacement of cations when the calcination temperature is higher than 800 °C.

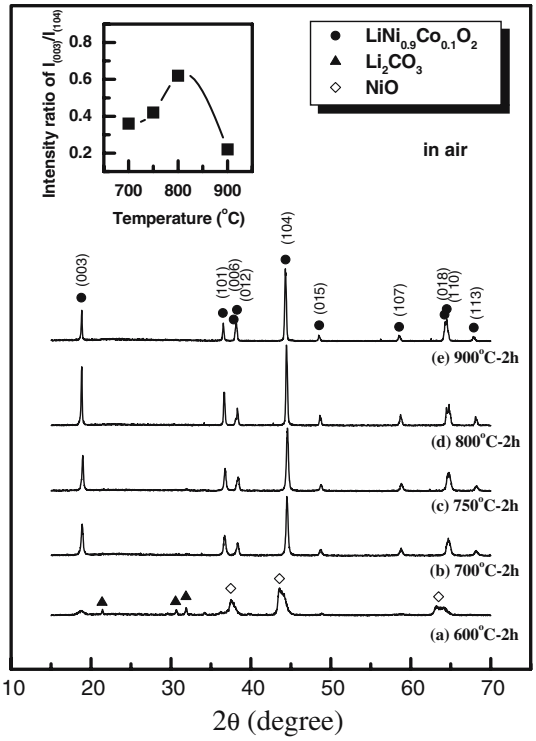

Fig. 2 XRD patterns of the microemulsion-derived powders calcined at (**a**) 600 °C, (**b**) 700 °C, (**c**) 750 °C, (**d**) 800 °C, and (**e**) 900 °C in air for 2 h. The inset refers the relation between the intensity ratio of I_{003}/I_{104} and the calcination temperature

Figure 3 shows the microstructural morphologies of the microemulsion-derived $LiNi_{0.9}Co_{0.1}O_2$ powders calcined at various temperatures in air. In Fig. 3(a) and (b), the average particle sizes of the 600 °C and 700 °C-calcined powders are 32 and 56 nm, respectively. Figure 3(c) displays the morphology of the 800 °C-calcined specimen. The average particle size is around 95 nm. In the conventional solid-state and sol–gel processes [21, 22], the particle sizes of lithium nickel cobalt oxide powders are in the range of 1–10 μm. Comparatively in this study, the particle sizes of the microemulsion-derived $LiNi_{0.9}Co_{0.1}O_2$ powders are significantly smaller. These results can be attributed to the specific characteristics of the microemulsion. In the microemulsion, nanosized

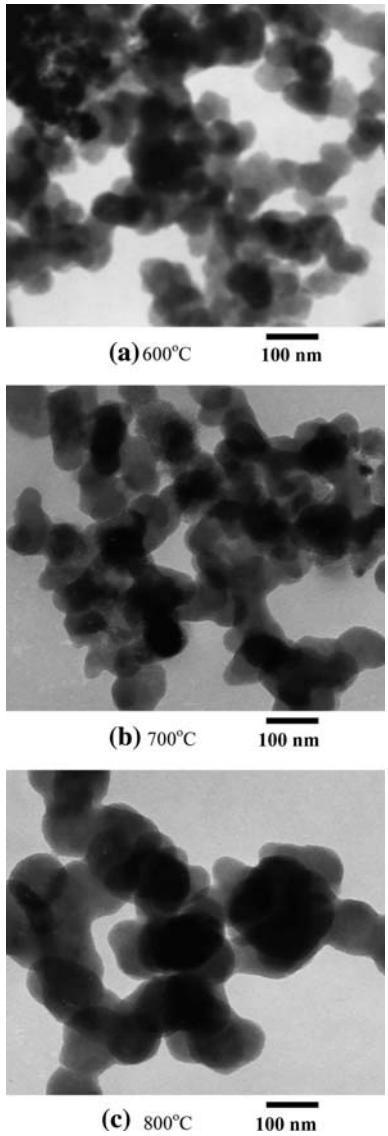

Fig. 3 TEM micrographs of the microemulsion-derived powders calcined at (**a**) 600 °C, (**b**) 700 °C, and (**c**) 800 °C in air for 2 h

reverse micelles are stabilized by the surfactant and co-surfactant molecules at the interface of the water and oil phases [15, 23]. These separated reverse micelles offer a unique microenvironment for the chemical reaction of the reactants to take place. In addition, these tiny micelles not only act as the nanoreactors, but also provide the steric barriers for the particles obtained after calcination [19]. Therefore, the aggregation among the formed particles during heating can be prevented, leading to the formation of nanosized powders.

Crystal structural analysis and microstructural observation of $LiNi_{0.9}Co_{0.1}O_2$ calcined in O_2

The oxygen content in the heating atmosphere is considered to be an important influential factor during the synthesis of $LiNi_{0.9}Co_{0.1}O_2$ powders having high cationic ordering. Figure 4 illustrates the XRD patterns for the specimens calcined in the range of 600–900 °C in O_2 for 2 h. The relative content of each observed phase was calculated by dividing the peak intensity of the strongest diffraction line of certain phase by the sum of the peak intensity of the strongest diffraction line of all observed phases. The variation of resultant phases versus the calcination temperature is illustrated in Fig. 5. It is shown that in Fig. 4(a) that the 600 °C-calcined powders contain Li_2CO_3 and NiO. When the calcination temperature is raised to 700 °C, well-crystallized powders are formed; furthermore, the intensity ratio of I_{003}/I_{104} is considerably greater than that of the specimen calcined in air. As the calcination temperature increases, a rise in the intensity ratio of I_{003}/I_{104} is observed. Once the heating temperature reaches 800 °C, monophasic $LiNi_{0.9}Co_{0.1}O_2$ powders are synthesized without other impurities and the intensity ratio of I_{003}/I_{104} increases to 1.35. These results confirm that well cation-ordered $LiNi_{0.9}Co_{0.1}O_2$ powders are successfully obtained. The lattice constants of the 800 °C-calcined powders are determined to be $a = 2.8751$ Å and $c = 14.1937$ Å, which are in consistency with those reported in literature [24]. The intensity ratio of I_{003}/I_{104} is 1.20 for the 900 °C-calcined specimen (see Fig. 4e). As shown in the inset of Fig. 4, heating at temperatures higher than 800 °C also leads to a decrease in the intensity ratio of I_{003}/I_{104}. This result is in accordance with that reported in the previous study [25]. The decrease in the I_{003}/I_{104} ratio arises from the displacement of lithium and nickel ions.

It is noted that the calcination time required for obtaining $LiNi_{0.9}Co_{0.1}O_2$ powders with high crystallinity via the microemulsion process is significantly decreased in comparison with those in other routes. For the solid-state process [26] and co-precipitation

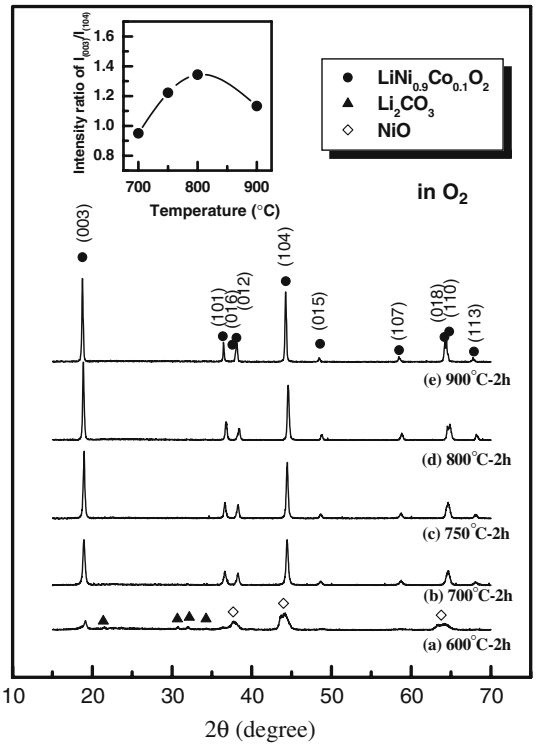

Fig. 4 XRD patterns of the microemulsion-derived powders calcined at (**a**) 600 °C, (**b**) 700 °C, (**c**) 750 °C, (**d**) 800 °C, and (**e**) 900 °C in O_2 for 2 h. The inset refers the relation between the intensity ratio of I_{003}/I_{104} and the calcination temperature

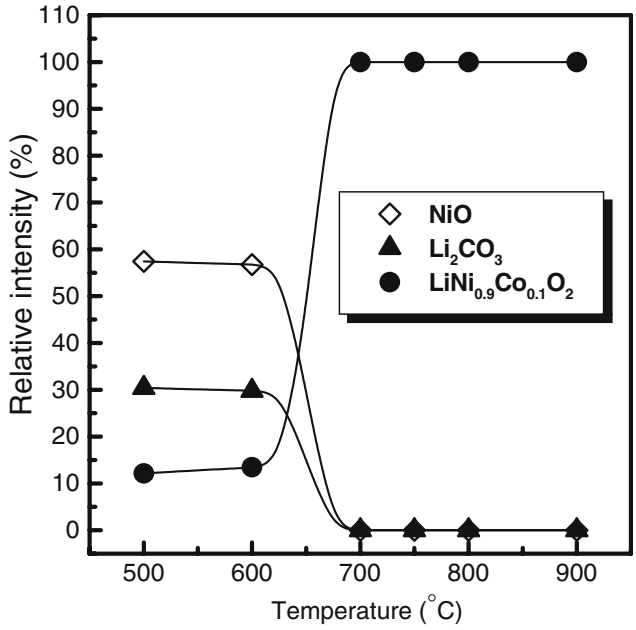

Fig. 5 Variations of resultant phases versus the calcination temperature for the microemulsion-derived $LiNi_{0.9}Co_{0.1}O_2$ powders

method [27], more than 10 h is required to synthesize the fully cation-ordered lithium nickel cobalt oxide powders; whereas, the required calcination time in the microemulsion process is considerably shortened to merely 2 h. The enhanced chemical reaction rate in the microemulsion process is due to the improved compositional homogeneity of the reactants in the nanosized micelles.

Figure 6 shows the TEM images of the microemulsion-derived $LiNi_{0.9}Co_{0.1}O_2$ powders. The average particle sizes of the powders calcined in pure O_2 at 600, 700, and 800 °C are 63, 106, and 127 nm, respectively. In comparison with the specimens calcined in air, the particle sizes of the $LiNi_{0.9}Co_{0.1}O_2$ powders calcined in pure O_2 are relatively large. These results suggest that oxygen content has a significant effect on the growth of the calcined powders. However, the particle size of the microemulsion-derived $LiNi_{0.9}Co_{0.1}O_2$ powders calcined in O_2 is still much smaller than those of the powders prepared via the solid-state process [28]. The particle size of the calcined powders poses critical impacts on the electrochemical characteristics [29, 30]. With prolonged calcination time, the obtained powders tend to aggregate to form large particles. The increase in the particle size lengthens the diffusion distance for lithium ions in the host structure, which is unfavorable to the intercalation and de-intercalation processes [29].

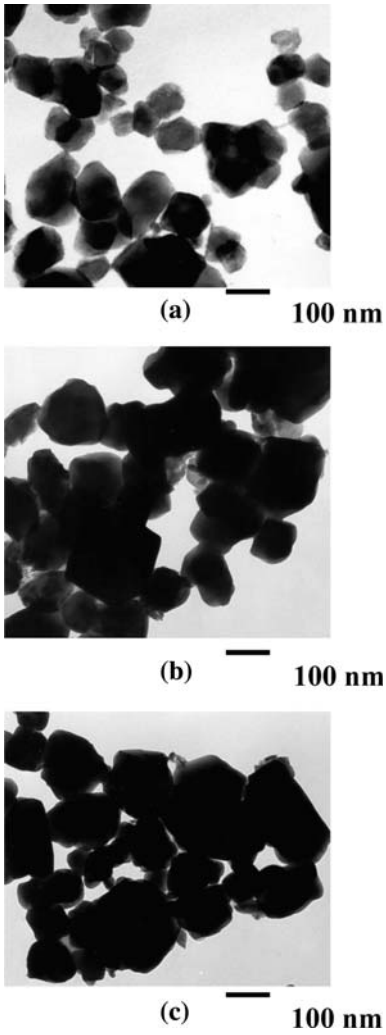

Fig. 6 TEM micrographs of the microemulsion-derived powders calcined at (**a**) 600 °C, (**b**) 700 °C, and (**c**) 800 °C in O_2 for 2 h

Electrochemical characterization of $LiNi_{0.9}Co_{0.1}O_2$ powders calcined in air and O_2

The charge and discharge curves of $LiNi_{0.9}Co_{0.1}O_2$ powders calcined at 800 °C in O_2 and air for 2 h are illustrated in Fig. 7(a) and (b), respectively. In Fig. 7(a), the specimen calcined in O_2 clearly displays a plateau at around 3.8 V in the discharging traces, which is in good accordance with the typical discharging behavior of $LiNi_{0.9}Co_{0.1}O_2$ observed in the previous study [13]. The specific discharge capacities in the first and the 20th cycles are 170.9 and 159.2 mAh/g, respectively. Figure 7(b) shows that the specific discharge capacities in the first and the 20th cycles for the specimen calcined in air are 159.4 and 110.0 mAh/g, respectively. The specific discharge capacity of the

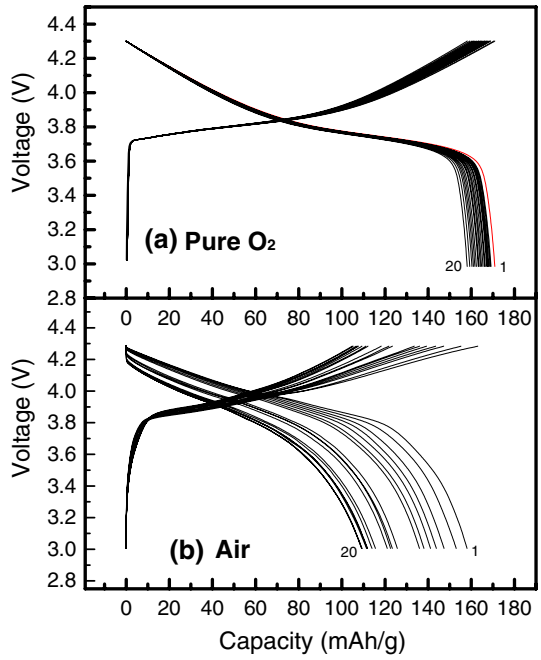

Fig. 7 Charge and discharge characteristics of the microemulsion-derived $LiNi_{0.9}Co_{0.1}O_2$ powders calcined (**a**) in pure O_2 and (**b**) in air between 4.3 V and 3.0 V at ambient temperature

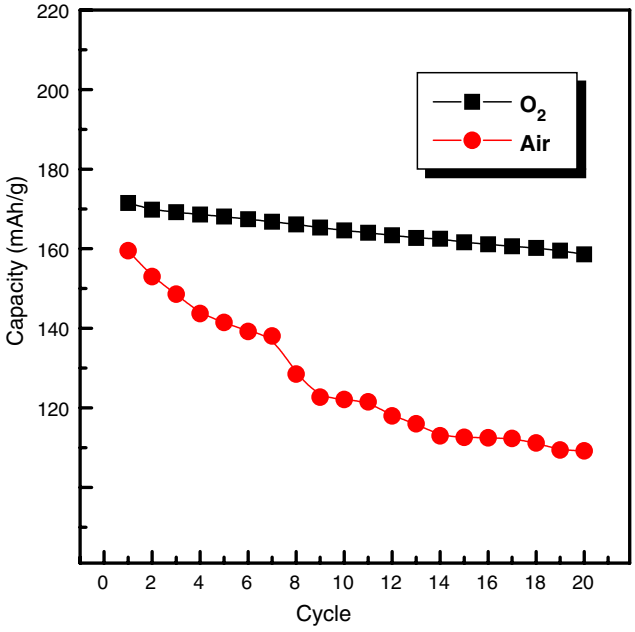

Fig. 8 Relations between the specific discharge capacities and the cycle number of the microemulsion-derived $LiNi_{0.9}Co_{0.1}O_2$ powders calcined in O_2 and in air

800 °C-calcined $LiNi_{0.9}Co_{0.1}O_2$ powders as a function of cycle numbers is depicted in Fig. 8. The capacity retention of $LiNi_{0.9}Co_{0.1}O_2$ powders calcined in O_2 is calculated to be 93.2% after 20 cycles; while, the powders calcined at 800 °C in air retains only 69% of the original capacity.

It is noted that the discharge capacity of the specimen calcined in air deteriorates significantly with an increase in the cycle number. The degradation of the cycling performance is owing to the low cationic ordering in the crystal structure, which can be evaluated based on the intensity ratio of I_{003}/I_{104} in the XRD patterns [1, 30]. From the variation of the intensity ratio of I_{003}/I_{104}, the displacement of lithium and transition metal ions can be identified. A high I_{003}/I_{104} ratio is beneficial to the electrochemical performance of the $R\bar{3}m$-structured compounds [21]. For $LiNi_{0.9}Co_{0.1}O_2$ powders calcined in O_2, most nickel and cobalt ions are regularly situated at the 3b sites regularly in the layered structure and lithium ions are located at the 3a sites, rendering the high cationic ordering that in turn facilitates the extraction/insertion of lithium ions [31] and suppresses the deterioration of the discharge capacity during cycling. It is revealed that $LiNi_{0.9}Co_{0.1}O_2$ powders with high specific discharge capacity and good cyclability can be successfully synthesized by performing the microemulsion process with appropriate calcination conditions.

Conclusions

Nanosized lithium nickel cobalt oxide ($LiNi_{0.9}Co_{0.1}O_2$) powders have been successfully prepared via the developed microemulsion process. The obtained powders are much smaller in size than those prepared via the conventional solid state and sol–gel processes. Oxygen has significant enhancement effects on the cationic ordering of the calcined powders. $LiNi_{0.9}Co_{0.1}O_2$ powders with high cationic ordering are synthesized at 800 °C in O_2 in this study. The electrochemical performance of the prepared powders is greatly influenced by the degrees of cationic ordering. The discharge capacities and capacity retention for $LiNi_{0.9}Co_{0.1}O_2$ calcined in O_2 are significantly improved. The microemulsion technique is demonstrated to be a promising route for synthesizing nanosized cathode materials with good electrochemical characteristics.

Acknowledgment The authors would like to thank the National Science Council, Taiwan, the Republic of China, for financial support of this study under Contract No. NSC 92-ET-7-002-003-ET.

References

1. Ohzuku T, Ueda A, Nagayama M (1993) J Electrochem Soc 140:1862
2. Chang CC, Kim JY, Kumta PN (2000) J Electrochem Soc 147:1722
3. Aydinol MK, Ceder G (1997) J Electrochem Soc 144:3832
4. Xia Y, Zhou Y, Yoshio M (1997) J Electrochem Soc 144:2593
5. Wang H, Jang YI, Chiang YM (1999) Electrochem Solid-State Lett 2:490
6. Ammundsen B, Paulsen J (2001) Adv Mater 13:943
7. Cho J, Jung H, Park Y, Kim G, Lim HS (2000) J Electrochem Soc 147:15
8. Li W, Currie JC (1997) J Electrochem Soc 144:2773
9. Gummow RJ, Thackeray MM (1993) J Electrochem Soc 140:3365
10. Chebiam RV, Prado F, Manthiram A (2001) J Electrochem Soc 148:A49
11. Madhavi S, Rao GVS, Chowdari BVR, Li SFY (2001) J Power Sources 93:156
12. Kweon HJ, Kim GB, Lim HS, Nam SS, Park DG (1999) J Power Sources 83:84
13. Caurant D, Baffier N, Garcia B, Ramos JPP (1996) Solid State Ionics 91:45
14. Lee KK, Yoon WS, Kim KB (2001) J Electrochem Soc 148:A1164
15. Gan LM, Liu B, Chew CH, Xu SJ, Chua SJ, Loy GL, Xu GQ (1997) Langmuir 13:6427
16. Zarur AJ, Ying JY (2000) Nature 403:65
17. Lu CH, Wang HC (2003) J Mater Chem 13:428
18. Ng WB, Wang J, Ng SC, Gan LM (1999) J Am Ceram Soc 82:529
19. Chang CL, Fogler HS (1997) Langmuir 13:3295

20. Ueda A, Ohzuku T (1994) J Electrochem Soc 141:2010
21. Cho J, Kim G, Lim HS (1999) J Electrochem Soc 146:3571
22. Andersson AM, Abraham DP, Haasch R, Maclaren S, Liu J, Amine K (2002) J Electrochem Soc 149:A1358
23. Pang YI, Bao X (2002) J Mater Chem 12:3699
24. Takahashi Y, Akimoto J, Gotoh Y, Kawaguchi K, Mizuta S (2001) J Solid State Chem 160:178
25. Yamada S, Fujiwara M, Kanda M (1995) J Power Sources 54:209
26. Saadoune I, Menetrier M, Delmas C (1997) J Mater Chem 12:2505
27. Cho J, Park B (2001) J Power Sources 92:35
28. Machida N, Maeda H, Peng H, Shiigematsu T (2002) J Electrochem Soc 149:A688
29. Lu CH, Wang HC (2003) J Eur Ceram Soc 23:865
30. Kim J, Amine K (2002) J Power Sources 104:33
31. Babu BR, Periasamy P, Thirunakaran R, Kalaiselvi N, Kumar TP, Renganathan NG, Raghavan M, Muniyandi N (2001) Int J Inorg Mater 3:401